# AFRL-SN-WP-TP-2006-121

# ANALYSIS OF A LEAKY TRAVELING WAVE ANTENNA (PREPRINT)

**Gregory M. Zelinski, Gary A. Thiele, M. Larkin Hastriter, Michael J. Havrilla, and Andrew J. Terzuoli**

**JULY 2006**

**STINFO COPY**

**SENSORS DIRECTORATE**
**AIR FORCE RESEARCH LABORATORY**
**AIR FORCE MATERIEL COMMAND**
**WRIGHT-PATTERSON AIR FORCE BASE, OH 45433-7320**

# REPORT DOCUMENTATION PAGE

| 1. REPORT DATE *(DD-MM-YY)* | 2. REPORT TYPE | 3. DATES COVERED *(From - To)* |
|---|---|---|
| July 2006 | Journal Article Preprint | 05/01/2004 – 05/01/2006 |

| 4. TITLE AND SUBTITLE | 5a. CONTRACT NUMBER |
|---|---|
| ANALYSIS OF A LEAKY TRAVELING WAVE ANTENNA (PREPRINT) | In-house |
| | **5b. GRANT NUMBER** |
| | |
| | **5c. PROGRAM ELEMENT NUMBER** N/A |

| 6. AUTHOR(S) | 5d. PROJECT NUMBER |
|---|---|
| Gregory M. Zelinski, M. Larkin Hastriter, Michael J. Havrilla, and Andrew J. Terzuoli (AFRL/AFIT) | 7622 |
| Gary A. Thiele (AFRL/SNDR) | **5e. TASK NUMBER** 11 |
| | **5f. WORK UNIT NUMBER** 0D |

| 7. PERFORMING ORGANIZATION NAME(S) AND ADDRESS(ES) | | 8. PERFORMING ORGANIZATION REPORT NUMBER |
|---|---|---|
| Air Force Institute of Technology (AFIT) Department of Electrical and  Computer Engineering Wright--Patterson AFB, OH 45433 | RF and EO Subsystems Branch (AFRL/SNDR) Aerospace Components & Subsystems Technology Division Sensors Directorate Air Force Research Laboratory, Air Force Materiel Command Wright-Patterson Air Force Base, OH 45433-7320 | AFRL-SN-WP-TP-2006-121 |

| 9. SPONSORING/MONITORING AGENCY NAME(S) AND ADDRESS(ES) | 10. SPONSORING/MONITORING AGENCY ACRONYM(S) |
|---|---|
| Sensors Directorate Air Force Research Laboratory Air Force Materiel Command Wright-Patterson Air Force Base, OH 45433-7320 | AFRL-SN-WP |
| | **11. SPONSORING/MONITORING AGENCY REPORT NUMBER(S)** AFRL-SN-WP-TP-2006-121 |

**12. DISTRIBUTION/AVAILABILITY STATEMENT**

**13. SUPPLEMENTARY NOTES**

**14. ABSTRACT**

Several leaky traveling wave antennas using the first microstrip higher order mode were simulated with the Finite Difference Time Domain (FDTD) method. The leaky wave antennas investigated here differ from previous designs. The propagation constant of each antenna was extracted from the resulting guided field distribution for comparison with a transverse resonance approximation, measured far-field patterns, and other simulated antennas. Variations of geometry were explored to investigate the complex propagation constant and its effect on the far-field pattern and the bandwidth.

**15. SUBJECT TERMS**

Antennas, traveling waves, leaky waves, Finite Difference Time Domain (FDTD), bandwidth

| 16. SECURITY CLASSIFICATION OF: | | | 17. LIMITATION OF ABSTRACT: | 18. NUMBER OF PAGES | 19a. NAME OF RESPONSIBLE PERSON (Monitor) |
|---|---|---|---|---|---|
| **a. REPORT** | **b. ABSTRACT** | **c. THIS PAGE** | SAR | 16 | Joshua Radcliffe |
| Unclassified | Unclassified | Unclassified | | | **19b. TELEPHONE NUMBER** *(Include Area Code)* N/A |

# Analysis of a Leaky Traveling Wave Antenna

Gregory M. Zelinski, *Student Member, IEEE,* Gary A. Thiele, *Life Fellow, IEEE,*
M. Larkin Hastriter, *Senior Member, IEEE,* Michael J. Havrilla, *Senior Member, IEEE,*
and Andrew J. Terzuoli, *Member, IEEE*

*Abstract*— Several leaky traveling wave antennas using the first microstrip higher order mode were simulated with the Finite Difference Time Domain (FDTD) method. The leaky wave antennas investigated here differ from previous designs. The propagation constant of each antenna was extracted from the resulting guided field distribution for comparison with a transverse resonance approximation, measured far-field patterns, and other simulated antennas. Variations of geometry were explored to investigate the complex propagation constant and its effect on the far-field pattern and the bandwidth.

*Index Terms*— Antennas, traveling waves, leaky waves, Finite Difference Time Domain (FDTD), bandwidth.

## I. INTRODUCTION

**M**ICROSTRIP antennas are attractive because of their light weight, low profile, and low cost. These antennas may be grouped into two classes: 1) the resonant patch, which is narrow band with a fixed main beam, and 2) the non-resonant leaky wave antenna, which typically has a wider bandwidth with a frequency-steerable main beam.

A leaky wave antenna must be excited by a higher order mode, since the fundamental mode of microstrip does not produce fields that decouple from the structure, as shown in Fig. 1(a). If the fundamental mode is not allowed to propagate, the next higher order mode may dominate above its cutoff frequency. Fig. 1(b) shows the electric field lines due to the first higher order mode $EH_1$. A phase reversal, or null, appears along the centerline that results in oppositely directed **E** fields at the edges allowing the fields to decouple and radiate.

In the late 1970's, Ermert [1], [2] was the first to publish the properties of higher order microstrip modes. However, his work was incomplete because his longitudinal propagation constant consisted solely of a phase constant $\beta$ but neglected the leakage constant $\alpha$. At about the same time, Menzel [3] published a paper on a microstrip transmission line antenna employing the first higher order mode. He assumed there was a meaningful leakage constant to allow the structure to radiate, but he did not recognize that he had developed a leaky
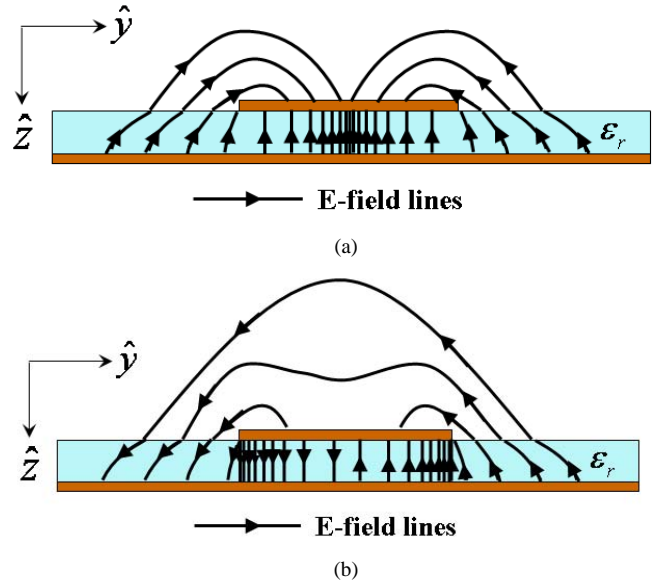
Fig. 1. (a) The electric field pattern associated with the fundamental mode of microstrip $EH_0$. (b) The electric field pattern associated with the first higher order mode of microstrip $EH_1$.

wave antenna and, thus, built it too short [4], [5]. Oliner [6] further clarified the fact that Menzel had actually built a leaky traveling wave antenna with a complex propagation constant.

Since the late 1970's there have been a number of papers on microstrip leaky wave propagation. Leaky wave propagation has been studied in [7]–[10] and leaky wave antennas in [11]–[17], although, the potential of these antennas has not been fully explored.

The performance parameters of a traveling wave antenna can be predicted as a function of the wavenumber in the direction of propagation within the structure. The guided wave phase constant $\beta$ determines the direction of the main beam from endfire, and the guided wave attenuation constant $\alpha$ determines the beamwidth of the main beam. Both constants together determine the leaky wave bandwidth. Walter [18] provided an excellent source for analysis of traveling wave antennas.

As seen in Fig. 2(a), Menzel's antenna uses seven slots cut from the conductor along the centerline to suppress the fundamental mode allowing leaky wave radiation via the first higher order mode. Fig. 2(b) shows an evolved antenna that incorporates a metal wall down the centerline to block the fundamental mode instead of transverse slots. Symmetry along this metal wall invites the application of image theory. One entire side of the antenna is now an image of the other side, making it redundant and unneeded. The resulting antenna in
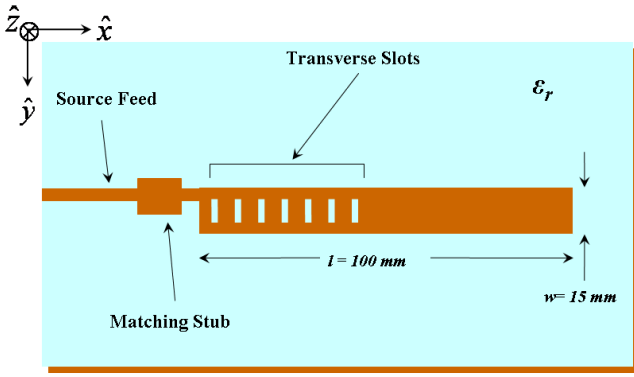
(a)



(b)



(c)

Fig. 2. (a) Menzel's original antenna [3], (b) the full width (FW) antenna, and (c) the half width (HW) antenna.



(a)



(b)

Fig. 3. A 2-D depiction of the 3-D computational space. (a) The $\hat{y} - \hat{z}$ slice of the FW antenna extending into the UPML (not to scale). The single source cell is marked by an X. The $\hat{x} - \hat{z}$ slice of Fig. 3(b) is outlined. (b) The $\hat{x} - \hat{z}$ slice of the FW antenna extending into the UPML (not to scale). The $\hat{y} - \hat{z}$ slice of Fig. 3(a) is outlined.

Fig. 2(c) is half the width of Menzel's antenna.

Advantages of the half width (HW) antenna compared to the Menzel antenna are: 1) no need to suppress the $EH_0$ mode; 2) no slot cross-polarized radiation that reduces radiation efficiency; 3) purer guided mode compared to the Menzel configuration, which improves radiation efficiency; 4) potentially less mutual coupling in an array environment.

## II. FDTD SIMULATION

### A. The computational domain

The three antennas of Fig. 2 were simulated for analysis. An FDTD algorithm [19] was used employing a 3-D central differencing Yee-cell formulation with a Uniaxial Perfectl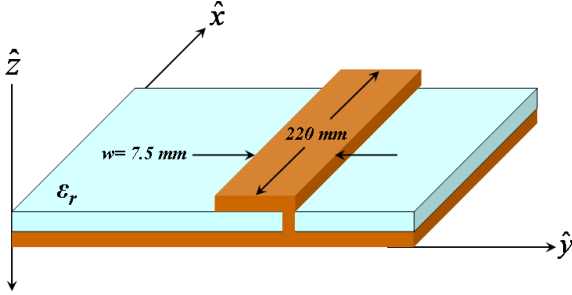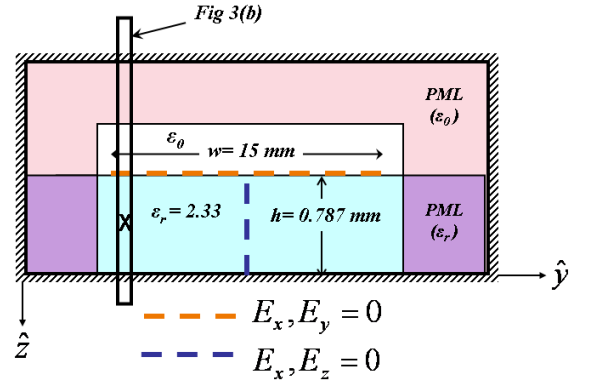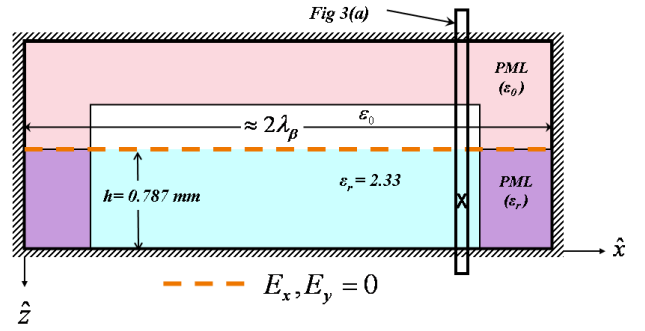y Matched Layer (UPML). The UPML was 10-cell-thick, 4th order polynomial graded, and PEC-backed on all six faces. The loss mechanism was normalized to free space to allow layers of unlike materials within the PML.

The copper conductor was modelled as a zero-thickness perfect electric conductor (PEC) by setting the tangential electric field to zero at the desired cell boundaries. Care was taken to accurately model the width of each antenna by reducing the PEC width by 1 cell, as demonstrated by Sheen [20].

The excitation means was a *hard* source with cubic growth over the first few periods to eliminate the problematic high frequency components of rapid transitions. A single source cell midway between the ground plate and the conductor strip, two cells inside from the open edge of the antenna and five cells from the PML created the best traveling wave distribution, although, nearly all contiguous geometries of source cells performed adequately.

To isolate the forward traveling wave, the reflections from the free space boundaries at the ends of the substrate needed to be eliminated. This was accomplished by extending the substrate directly into the UPML, and modifying the affected UPML cells to match the substrate. The resulting grid space for the full width (FW) antenna is seen in Fig. 3. The UPML absorbs all outward propagating waves in the substrate allowing the forward traveling wave to develop exclusively.

Convergence of the extracted wavenumber was maintained while reducing the substrate thickness to only five cells and elongating the cells in the $\hat{x}$ direction to a size of 3:1:1.
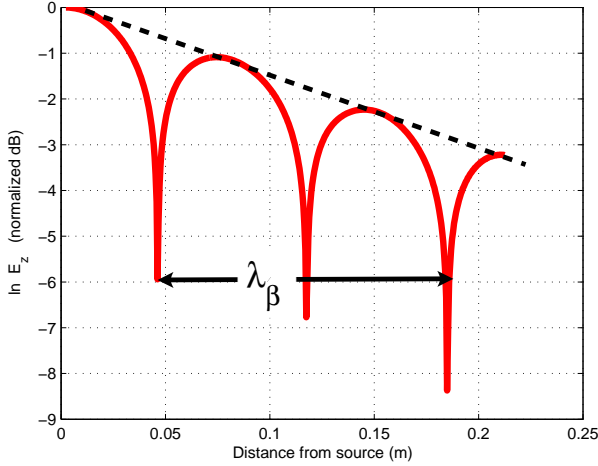
Fig. 4. The natural logarithm of the simulation data was used to determine the propagation constant.

Resolution within the structure was well over 100 cells per wavelength for all trials. The substrate modelled, Rogers Duroid 5870 high frequency laminate, has a loss tangent of only 0.0012. Neglecting this loss showed no noticeable effect on the extracted propagation constant. To further reduce memory demands of the largest simulations, single precision was used resulting in approximately 40% decrease in memory usage. These parameters allowed simulations to be accurately run on a personal computer with only 1 GB of RAM.

### B. Determination of $\alpha$ and $\beta$

The objective of the FDTD simulations was to provide the propagation constant of the vertical component of the electric field $E_z$ inside the substrate between the top conductor and the bottom ground plate. The $E_z$ data was retrieved from a single row of cells stretching the length of the antenna in the $\hat{x}$ direction. The logarithm of the normalized magnitude of the $\hat{z}$-directed electric field from these cells created a waveform from which $\alpha$ and $\beta$ were extracted using:

$$E_z = e^{(\alpha - j\beta)x}$$
$$\ln E_z = \alpha x - j\beta x \quad (1)$$

As shown in Fig. 4, $\alpha$ is the slope of the peaks of $\ln E_z$ (shown as a dotted line) and $\beta$ is found from the separation of nulls using:

$$\beta = \frac{2\pi}{\lambda_\beta} \quad (2)$$

If the simulation is run long enough to ensure steady state (the traveling wave distribution has a constant wavelength), only $\lambda_\beta/2$ is needed for determination of the wavenumber.

### C. Transverse resonance approximation

For comparison, a transverse resonance approximation was created following the work of Oliner and Lee [4], [21] which
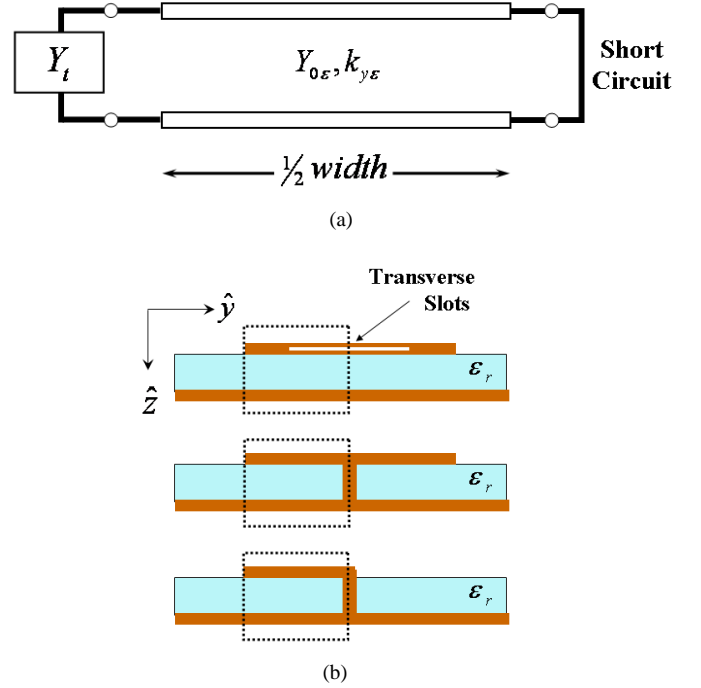


Fig. 5. (a) is a transmission line circuit that approximates the cross section of each of the three structures in (b) operating in mode EH$_1$. The cross sections in (b) represent Menzel (top), FW (center), and HW (bottom).

they confirmed with a steepest descent contour analysis. Fig. 5 shows a transmission line model that is applicable to the cross section of the Menzel, FW, and HW antennas. Each structure can be modelled as a dielectric-filled parallel plate waveguide of admittance $Y_{0\varepsilon}$ terminated at one end by a short circuit and the other end by admittance $Y_t$. The **E** null generated in the EH$_1$ mode by a vertical wall or transverse slots is represented by a short circuit. $Y_t$ is an approximation of the admittance of an open edge of microstrip developed by Chang and Kuester [22], [23] using the Weiner-Hopf technique to analyze a TEM wave that is completely reflected.

The transverse resonance relation:

$$\Gamma_{right}(y) \cdot \Gamma_{left}(y) = 1 \quad (3)$$

must hold for all points in the transverse $\hat{y}$ direction.

The reflection coefficient $\Gamma$ due to the admittance of the end of the microstrip $Y_t$ is unity with a phase shift $\chi$, as defined in [22], [23]. At a point $y = y_a$ just to the right of $Y_t$,

$$\Gamma_{right}(y_a) = -e^{-j2k\frac{w}{2}} \quad (4)$$
$$\Gamma_{left}(y_a) = e^{j\chi} \quad (5)$$

where $k = \beta - j\alpha$ is the complex wavenumber in the substrate and $w$ is the width of the structure. Eq. (3) becomes:

$$-e^{-jkw} \cdot e^{j\chi} = 1$$
$$\chi - kw = \pm n\pi \quad n = 1, 3, 5, \ldots \quad (6)$$
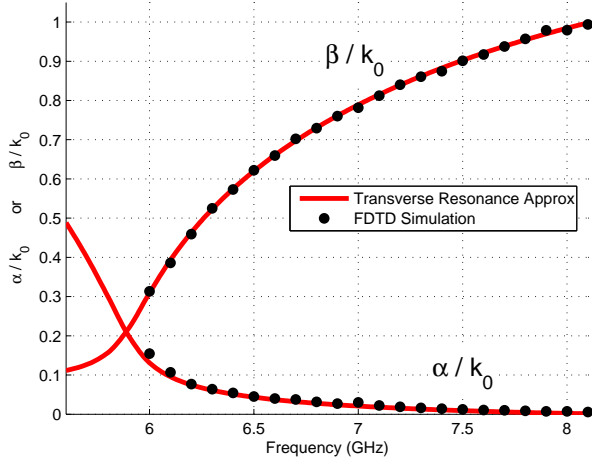
$n = 1$ for the EH$_1$ mode.

Fig. 6.   The FDTD simulation of the HW is in agreement with the transverse resonance approximation.

Fig. 6 shows that the transverse resonance approximation is in agreement to within $1\%$ of the FDTD-derived $\beta$ data over the entire leaky band.

## III. RESULTS

### A. Similarities/Differences between HW, FW, Menzel

Generally our simulated and measured results showed the HW antenna to have advantages over the FW antenna and Menzel antenna. At most leaky-band frequencies, the Menzel configuration used here had noticeably larger cross-polarization (e.g. 10 dB at 6.2 GHz decreasing to 2 dB at 7.7 GHz) in the far-field as typified by the measurements in Fig. 7(a). This is due in part to radiation by the non-resonant slots used to suppress the fundamental mode in the Menzel configuration. The cross-pol energy from the Menzel slots leads to decreased co-pol gain measurements, as indicated in Fig. 7(b). The co-pol decrease of the Menzel configuration is typically on the order of 3 dB, although Fig. 7(b) shows an even greater reduction at 7.2 GHz. Further, the FDTD simulations show that the slots in the Menzel design are not as effective in keeping the fundamental mode suppressed as is the long wall in the FW and HW antennas.

The co-pol measurements showed the HW has a slightly different mainbeam location and an increased backlobe. This is due to an uncertainty in the HW fabricated model as to its effective width since the vias are of finite diameter and merely approximate a solid wall. The effective width significantly affects $\alpha$ and $\beta$ [24]. Slightly reducing the width of the HW by 0.15 mm matched the $\alpha$ and $\beta$ of the FW and Menzel antennas seen in Fig. 7(b).

Our simulated results confirmed that $\alpha$ and $\beta$ of the FW and HW antennas were the same, as anticipated by image theory. Further, the FW antenna induced fields in the passive side that degraded the $180^0$ phase difference across the width of the antenna [24]. This resulted in decreased radiation efficiency (i.e., reduced measured gain) for the FW antenna relative to a HW antenna with the same $\beta$, as evidenced in Fig. 7(b).
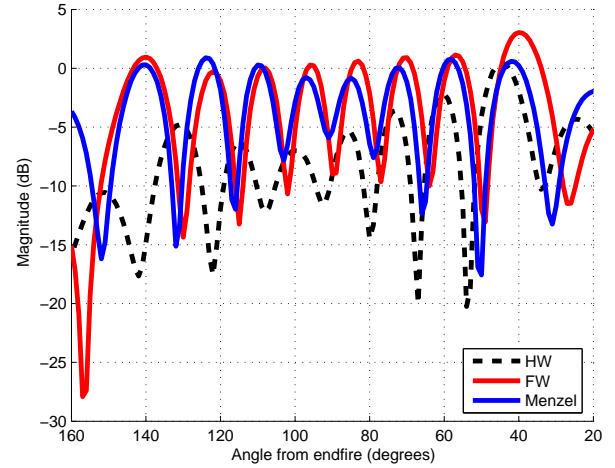


(a)
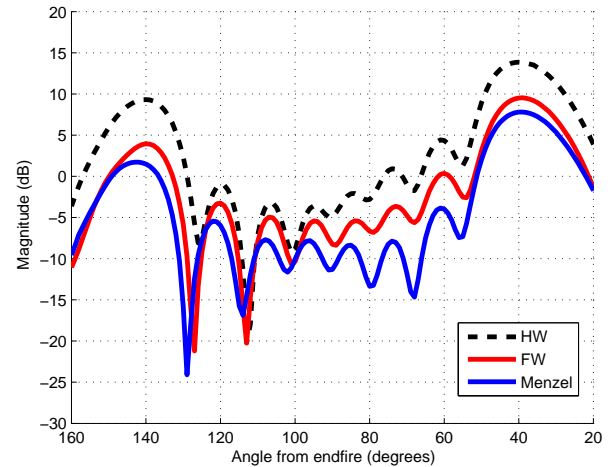


(b)

Fig. 7.   (a) Cross-polarized and (b) Co-polarized measured far-field patterns of the HW, FW, and Menzel antennas at 7.2 GHz.

### B. Limitations of the Transverse Resonance approximation

The transverse resonance model was useful to get a quick approximation; however, a new model would be needed for geometries other than those in Fig. 2. In addition, the $Y_t$ approximation is not valid when the microstrip is curved or tapered.

Kuester, et al [23] state applicability to only *thin* substrates in which:

$$h \ll \frac{1}{\omega} \frac{1}{\sqrt{\varepsilon\mu}} \qquad (7)$$

For a substrate thickness $h = 787\mu$m, Eq. (7) requires frequencies $\ll$ 40 GHz, which is five times higher than the highest frequency of this leaky band. Fig. 8(a) shows that FDTD and transverse resonance begin to disagree as the height of the substrate increases past the *thin* criteria of Eq. (7), near $h$= 1.1 mm at 6.7 GHz.

## C. Modifying dimensions to meet bandwidth specifications

The leaky bandwidth is defined by $\alpha = \beta$ at the lower end and $\beta = k_0$ at the upper end. Bandwidth around a desired center frequency $f_c$ can be achieved by scaling the width of the conducting strip, the height (or thickness) of the substrate, and/or the permittivity of the substrate. The bandwidth can be increased, to a limited extent, by the selection of the substrate material. As a fraction of the center frequency, the percent bandwidth will be unaffected by altering the height and width, although $f_c$ can be readily shifted. The choice of substrate material and thickness is usually dictated by cost or availability of material, therefore, the width is typically the parameter to manipulate.

Fig. 8(a) illustrates the relationship between the height, or thickness, of the substrate and the propagation constant. Like permittivity, the height of the substrate is usually dictated by the material available. All antennas simulated and fabricated for this work used material that was 787 $\mu$m thick. As mentioned in the previous section, the transverse resonance solution includes an approximation that limits its applicability to thin substrates. The difference in $\beta$ between FDTD and transverse resonance becomes noticeable for heights greater than approximately 1.1 mm.

Fig. 8(b) shows that the propagation constant is very sensitive to the width of the conductor strip. As little as 0.1 mm difference in width will cause as much as $10\%$ error in $\beta$. This sensitivity to width requires adequate fabrication precision.

Fig. 8(c) illustrates the relationship between the relative permittivity of the substrate and the propagation constant. Fig. 9 shows the bandwidth as a function of substrate permittivity overlayed with common substrates. Bandwidth increases rapidly as the substrate dielectric constant nears that of free space. Fig. 10 shows the drawback of lower dielectric constant substrate is a very low $\alpha$ across most of the leaky band. Low $\alpha$ results in little energy radiating per unit length.

The leaky frequency band can be scaled up or down by scaling the width and height inversely while using the same permittivity. For example, Table I shows the effect on frequency by halving the height and width. While the bandwidth appears to double, the effective bandwidth remains the same percentage of the center frequency $f_c$.

TABLE I
SCALING THE FREQUENCY BY A FACTOR OF TWO.

| Bandwidth | 2.4 GHz | 4.8 GHz |
|---|---|---|
| $f_c$ | 7.08 GHz | 14.16 GHz |
| $w$ | 15 mm | 7.5 mm |
| $h$ | 787 $\mu$m | 393.5 $\mu$m |
| $\varepsilon_r$ | 2.33 | 2.33 |

Frequency scaling does not prove useful for reduction of the FDTD simulation since cross section ratio of height to width is unchanged. However, this property could be useful to shrink the antenna to meet measurement facility size constraints. Conversely, fabrication may be made easier by increasing the size of the antenna.
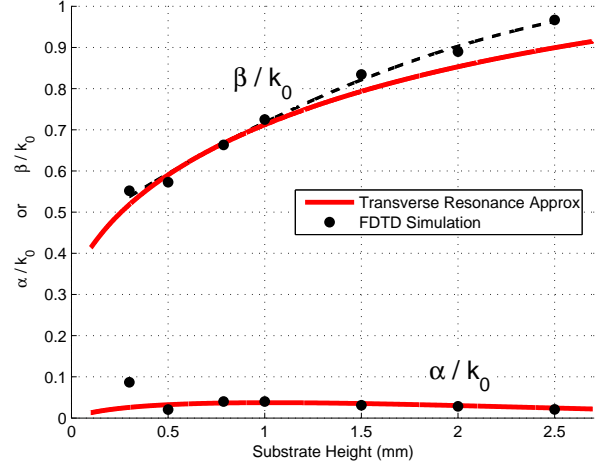


(a)
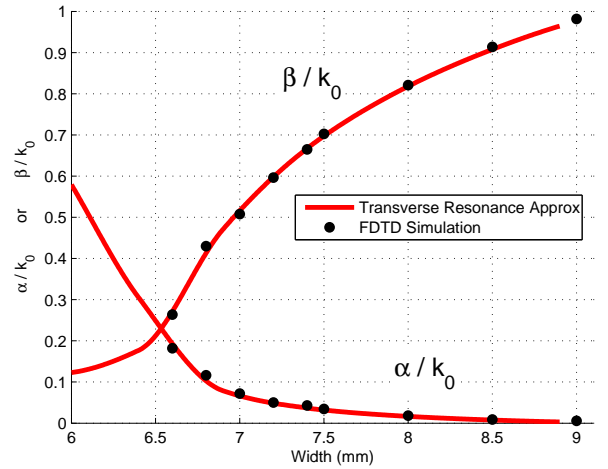


(b)
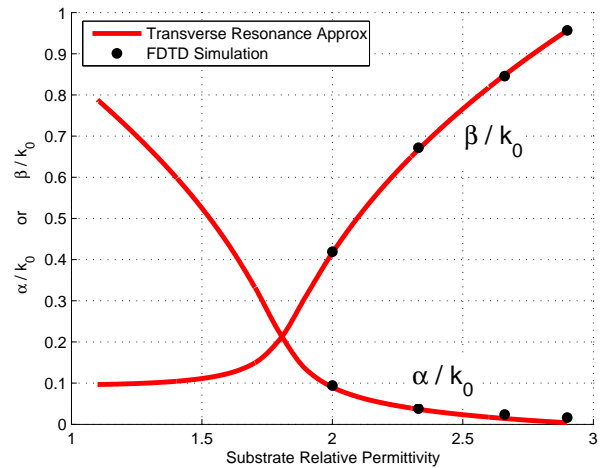


(c)

Fig. 8.   The parameters of the HW antenna are $h = 787\mu$m, $\varepsilon_r = 2.33$, and $w = 7.5$ mm. Shown are the effects at 6.7 GHz of varying the (a) height, (b) conductor width, and (c) permittivity with the other parameters unchanged. The dashed line in (a) is a quadratic least square of the FDTD data points.
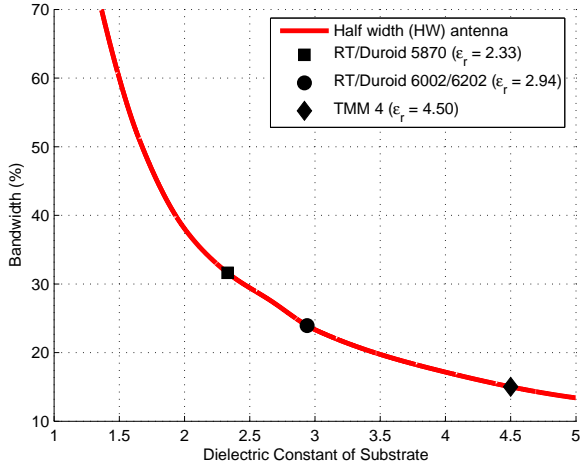
Fig. 9. The bandwidth as a function of substrate permittivity for the HW antenna (h = 0.787 mm; w = 7.5 mm.) Three common, commercially-available substrates are overlayed



Fig. 11. The $180^0$ curve simulated with the wall on the inside of the curve. The source cell is marked by the $X$ in the lower left of the figure. The guided traveling wave was extracted from the cells marked by the dotted line along the open edge using angular position $\theta$ with respect to the source cell.

TABLE II
SUMMARY OF CURVATURE TRIALS.

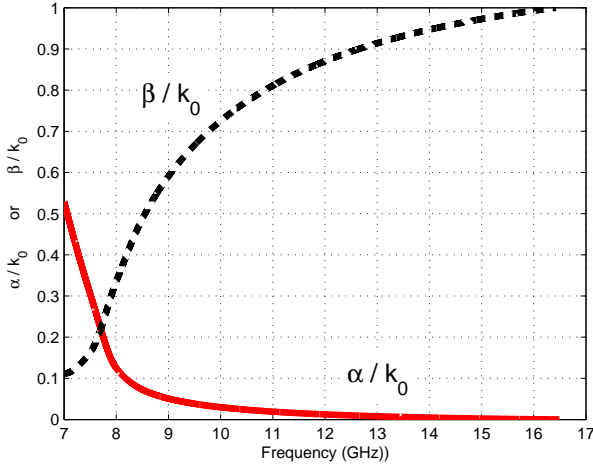|  | $180^0$ | $180^0$ | $180^0$ | $90^0$ | straight |
|---|---|---|---|---|---|
| Radius(cm) | 3.36 | 4.23 | 5.32 | 9.3 | $\infty$ |
| Arc length (cm) | 10.6 | 13.3 | 16.7 | 14.6 | N/A |
| Largest $\lambda_\beta$ possible (cm) | 21.2 | 26.6 | 33.4 | 29.2 | N/A |
| Lowest $f$ possible (GHz) | 6.2 | 6.1 | 6.0 | 6.1 | N/A |
| Approx Bandwidth (GHz) | 2.8 | 2.7 | 2.6 | 2.5 | 2.3 |

a $180^0$ arc of radius 4.23 cm produces destructive interference indicating the presence of one or more other modes.

### E. Effect of multiple elements on $\alpha$ and $\beta$

The main beam of a traveling wave antenna is frequency steerable in the longitudinal direction from near endfire to near broadside. A linear array of HW elements is able to scan in two dimensions. A first step to developing such an array is to determine the effect of spacing between neighboring elements. Two elements were simulated next to each other at 7.2 GHz. The results were nearly identical regardless of whether the second element was excited or not. The impact on the propagation constant by a neighboring element is shown in Fig. 14. There is minimal interaction between elements if they are separated by at least $0.25\lambda$ and virtually no interaction if the spacing is over $0.4\lambda$.



Fig. 10. The normalized $\alpha$ and $\beta$ curves in the leaky band for the HW antenna using substrate with $\varepsilon_r$=1.33 (h = 0.787 mm; w = 7.5 mm.)

### D. Effect of curvature on $\alpha$ and $\beta$

Shown in Fig. 11 is a curved HW antenna with its wall along the inside edge. Simulations were done at radii of 3.36, 4.23, 5.32, and 9.3 cm. $180^0$ was simulated when possible. Only $90^0$ was simulated for the largest simulation due to availability of computing resources. The size of the computational domain of all curved simulations necessitated only single precision. The cell size 1.5:1.5:1 was used for all curved HW trials. Not enough information is available to extract the wavenumber for frequencies whose $\lambda_\beta$ is greater than twice the length of the arc. The curvature trials are summarized in Table II. Fig. 12 shows that curvature increases bandwidth by flattening $\beta$, predominantly for the lower frequencies, while keeping $\alpha$ relatively unaffected. As the radius of curvature decreases, the bandwidth increases.

Curvature with the wall on the outside hampers the ability of the antenna to set-up only the $EH_1$ mode. As seen in Fig. 13,
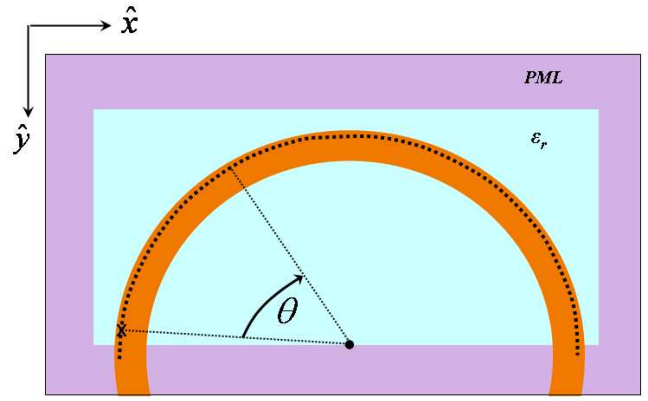
### IV. CONCLUSION

A three dimensional FDTD simulation was constructed to simulate various leaky wave microstrip antennas. FDTD was shown to be able to extract the complex guided wavenumber, which is useful in predicting antenna performance measures such as bandwidth, beamwidth, and main beam direction. The antenna geometry was easily manipulated in FDTD to meet various testing requirements of different structures. Several means were found to decrease the number of cells required to accurately simulate the antennas allowing elaborate simulations with only a standard desktop PC with 1 GB of memory. High performance computing resources, which are typically required for such modelling, were not used.

(a)



(a)



(b)



(c)



(b)

Fig. 13. Curvature with the wall on the *outside* produces field distributions, seen here at (a) 6.4 GHz and (b) 7.4 GHz, that suggest the presence of multiple modes.
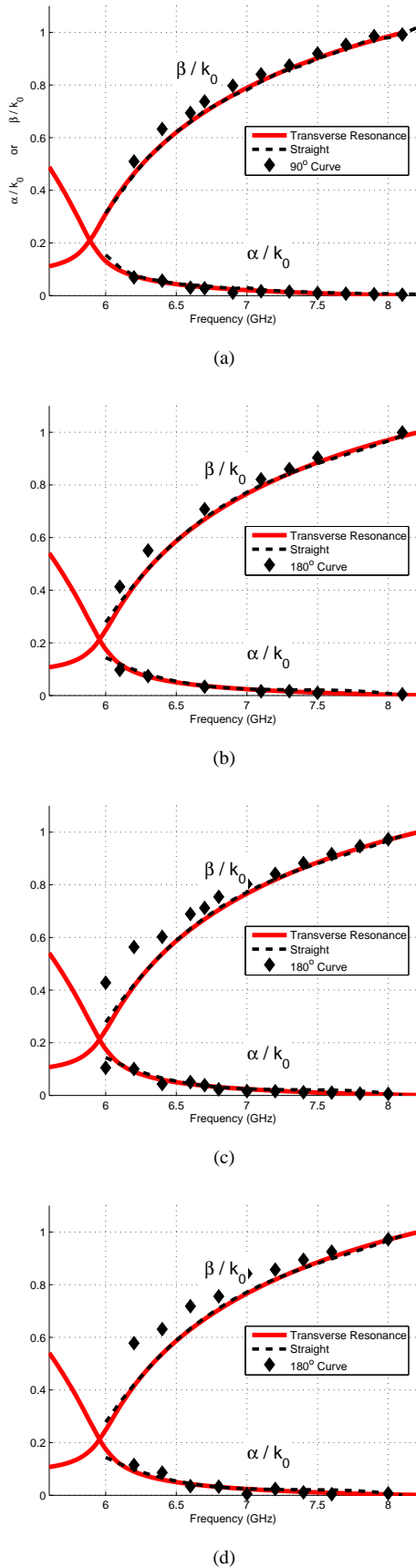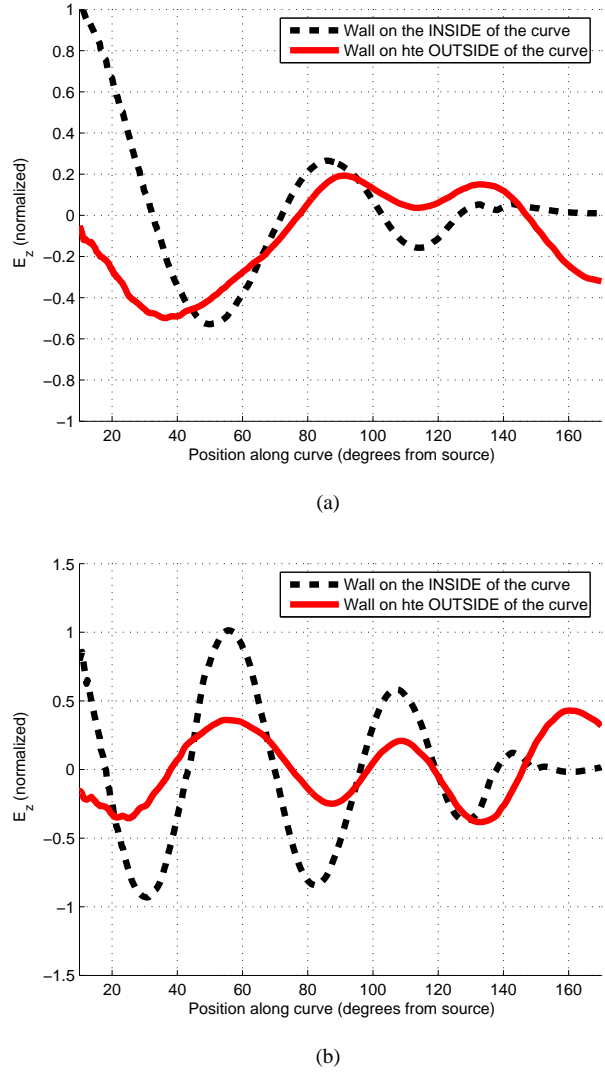


(d)

Fig. 12. The curved HW antenna with a radius of (a) 93 mm, (b) 53 mm, (c) 42 mm, and (d) 34 mm. For comparison, the single precision *curved* data is plotted alongside the single precision *straight* data.

The HW antenna was shown to be an improvement over both the FW antenna as well as the Menzel antenna. The propagation constant of the HW antenna behaved equivalently to the FW antenna as anticipated by image theory. In addition, the non-excited side of the FW antenna was shown to degrade the $180^0$ phase difference across the structure's width thereby decreasing the radiation efficiency. The vertical wall of the HW antenna was found to be more capable of blocking the fundamental mode than the slots in the antenna developed by Menzel.

Two HW antenna elements were excited in close proximity to test mutual interaction. No effect to the propagation constant of elements was observed if the spacing distance was greater than $0.4\lambda$. This lack of mutual coupling will simplify array designs.

The effect of curvature on the complex propagation constant of the HW antenna was investigated. As a function of curvature, no significant impact to $\alpha$ was noticed, however, the $\beta$ plot showed significant flattening, particularly at lower
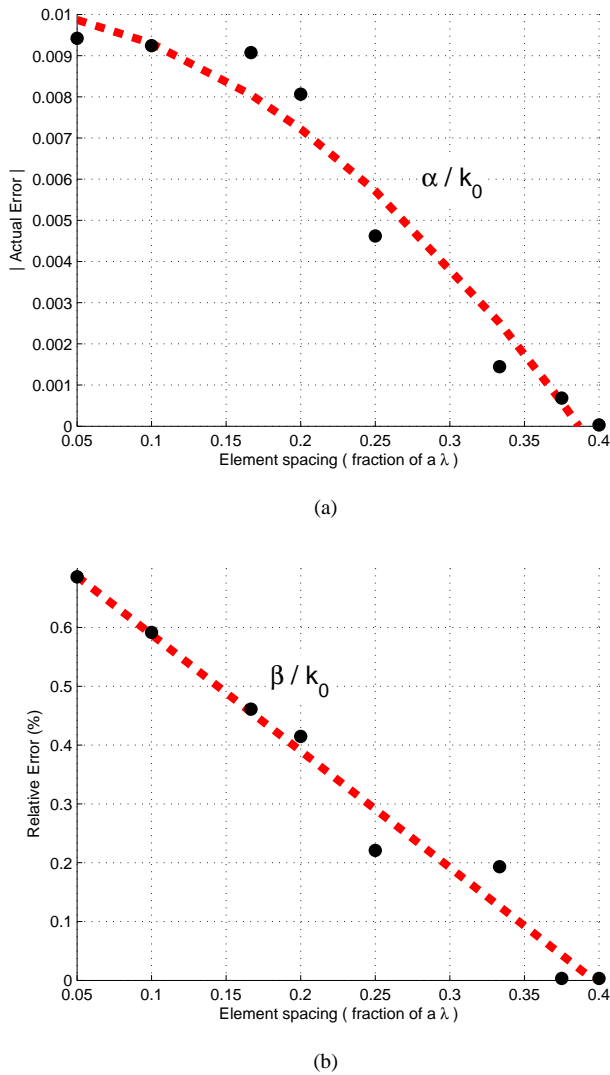
(a)



(b)

Fig. 14.   (a) Actual error of $|\alpha|$ (dashed line is quadratic least square) and (b) relative error of $\beta$ (dashed line is linear least square) from placing another element a fraction of a wavelength from the open end of the antenna. For both figures, the error is with respect to the guided wavenumber of a single element.

frequencies. Flattening $\beta$ without affecting $\alpha$ results in a bandwidth increase.

The bandwidth of the HW antenna can be increased by using a lower permittivity dielectric constant; however, a commercially available substrate could not be found lower than 2.2. Lowering the dielectric constant has the drawback of a very low $\alpha$ across much of the leaky band, which hinders the antenna's ability to efficiently radiate. Varying the width of the conducting strip or the height of the substrate were found to move the center frequency but did not change the bandwidth as a percentage of center frequency. The width and height can be varied together to scale the center frequency.

## ACKNOWLEDGMENT

## REFERENCES

[1] H. Ermert, "Guided modes and radiation characteristics of covered microstrip lines," *Archiv fur Elektronik und Ubertragungstechnik (AEU)*, vol. 30, no. 2, pp. 65–70, April 1976.

[2] ——, "Guiding and radiation characteristics of planar waveguides," *Microwaves, Optics, and Acoustics*, vol. 3, no. 2, pp. 59–62, March 1979.

[3] W. Menzel, "A new travelling-wave antenna in microstrip," *Archiv fur Elektronik und Ubertragungstechnik (AEU)*, vol. 33, no. 4, pp. 137–140, April 1979.

[4] A. A. Oliner and K. S. Lee, "The nature of the leakage from higher modes on microstrip line," *IEEE MTT-S International Microwave Symposium Digest*, pp. 57–60, 1986.

[5] ——, "Microstrip leaky wave strip antennas," *Proceedings of the Antennas and Propagation Society International Symposium*, vol. 24, pp. 443–446, June 1986.

[6] A. A. Oliner, "Leakage from higher modes on microstrip line with applications to antennas," *Radio Science*, vol. 22, no. 6, pp. 907–912, November 1987.

[7] J. S. Bagby, D. P. Nyquist, C.-H. Lee, and Y. Yuan, "Identification of propagation regimes on integrated microstrip transmission lines," *IEEE Transactions on Microwave Theory and Techniques*, vol. 41, no. 11, pp. 1887–1894, November 1993.

[8] S.-D. Chen and C.-K. C. Tzuang, "Characteristic impedance and propagation of the first higher order microstrip mode in frequency and time domain," *IEEE Transactions on Microwave Theory and Techniques*, vol. 50, no. 5, pp. 1370–1379, May 2002.

[9] Y.-D. Lin and J.-W. Sheen, "Mode distinction and radiation efficiency analysis of planar leaky-wave line source," *IEEE Transactions on Microwave Theory and Techniques*, vol. 45, no. 10, pp. 1540–1543, October 1997.

[10] F. Mesa, D. R. Jackson, and M. J. Freire, "Evolution of leaky modes on printed-circuit lines," *IEEE Transactions on Microwave Theory and Techniques*, vol. 50, no. 1, pp. 94–104, January 2002.

[11] D. R. Jackson and A. A. Oliner, "A leaky-wave analysis of the high-gain printed antenna configuration," *IEEE Transactions on Antennas and Propagation*, vol. 36, no. 7, pp. 905–910, July 1988.

[12] D. Janning and G. A. Thiele, "Conformal microstrip leaky wave antenna," U.S. Patent Application, February 9, 2005.

[13] W. Hong, T.-L. Chen, C.-Y. Chang, J.-W. Sheen, and Y.-D. Lin, "Broadband tapered microstrip leaky-wave antenna," *IEEE Transactions on Antennas and Propagation*, vol. 51, no. 8, pp. 1922–1928, August 2003.

[14] C.-N. Hu, C.-K. Tzuang, and S.-D. Chen, "A novel design for the microstrip leaky-mode antenna array with high efficiency," *IEEE Transactions on Microwave Theory and Techniques*, vol. 41, no. 11, pp. 247–250, 21-25 May 2000.

[15] V. Nalbandian and C. S. Lee, "Bandwidth enhancement of microstrip antenna with leaky-wave excitation," *1999 IEEE Antennas and Propagation Society International Symposium*, vol. 2, pp. 1224–1227, 11-16 July 1999.

[16] ——, "Tapered leaky-wave ultrawide-band microstrip antenna," *1999 IEEE Antennas and Propagation Society International Symposium*, vol. 2, pp. 1236–1239, 11-16 July 1999.

[17] C.-K. C. Tzuang, "Leaky-mode perspective on printed antenna," *Proceedings of the National Science Council, Republic of China*, vol. 23, no. 4, pp. 544–548, May 1999.

[18] C. H. Walter, *Traveling Wave Antennas*.  New York, NY: McGraw-Hill, 1965.

[19] A. Taflove and S. Hagness, *Computational Electrodynamics: The Finite Difference Time-Domain Method*, 2nd ed.  Boston, MA: Artech House, 2000.

[20] D. M. Sheen, "Numerical modeling of microstrip circuits and antennas," Ph.D. dissertation, Massachusetts Institute of Technology, Cambridge, MA, 1991.

[21] K. S. Lee, "Microstrip line leaky wave antennas," Ph.D. dissertation, Polytechnic Institute of New York, 1986.

[22] D. C. Chang and E. F. Kuester, "Total and partial reflection from the end of a parallel-plate waveguide with an extended dielectric slab," *Radio Science*, vol. 16, no. 1, pp. 1–13, January-February 1981.

[23] E. F. Kuester, R. T. Johnk, and D. C. Chang, "The thin-substrate approximation for reflection from the end of a slab-loaded parallel-plate waveguide with applications to microstrip patch antennas," *IEEE Transactions on Antennas and Propagation*, vol. AP-30, no. 5, pp. 910–917, September 1982.

[24] G. M. Zelinski, "Finite difference time domain analysis of a leaky traveling wave microstrip antenna," Master's thesis, Air Force Institute of Technology, Wright-Patterson AFB, OH, March 2005.

**Gregory M. Zelinski** (S'99-M'01) received the BSEE from Wright State University, Dayton, OH, in 2000 and the MSEE from the Air Force Institute of Technology, Wright-Patterson AFB, OH in 2005.

From 2001-2003, he was a flight test engineer in the 339th Flight Test Squadron, Robins AFB, GA, where he managed the test and evaluation of sustainment modifications to nearly all current configurations of C-5, C-141, and C-130 aircraft in the United States Air Force inventory. Currently, he is a project engineer in the Sensors Directorate of the Air Force Research Laboratory, Wright-Patterson AFB, OH.

**Gary A. Thiele** (S'58-M'61-SM'74-F'82-LF'03) was born in Cleveland, Ohio, on May 5, 1938. He received the B. S. degree in electrical engineering from Purdue University, Lafayette, IN, in 1960, and the M.Sc. and Ph.D. degrees in electrical engineering from The Ohio State University, Columbus, OH in 1964 and 1968, respectively.

From 1960 to 1961, Dr. Thiele was with the General Electric Company and from 1961 to 1962, he served as an officer in the U.S. Army Signal Corps. From 1969 to 1980, he was a member of the faculty at The Ohio State University and a member of the OSU ElectroScience Laboratory. During 1976 he was a Visiting Fellow at the University of New South Wales, Canberra, Australia. In January 1980, he became Associate Dean and Director of Graduate Studies and Research in the School of Engineering at the University of Dayton, where he was the founding Director of the Electro-Optics Graduate Program. In August 1991 he assumed the F. M. Tait Chair in Engineering until his retirement from the university in 2001. From June 1993 to August 1994, while on sabbatical, he was a Visiting Scientist at Wright-Patterson AFB and during the autumn of 1994 a Visiting Distinguished Lecturer at the Air Force Institute of Technology. Prof. Thiele is the author of "Wire Antennas" in the text Computer Techniques for Electromagnetics (Pergamon, 1973) and is coauthor of the popular textbook Antenna Theory and Design (Wiley, 1981, 1998). His technical interests include antennas, radar cross section, electromagnetic compatibility, electromagnetic phenomena, and computational methods in electromagnetic theory.

Prof. Thiele co-received the 1975 Best Paper Award for a contribution to the IEEE Transactions on Antennas and Propagation. He was elected to a three-year term as a member of the AP-S Administrative Committee for the years 1976-1978. He also served the Antennas and Propagation Society as Secretary/Treasurer (1978-1980), as Vice President (1981), and as President (1982). Dr. Thiele was elected a Fellow of the IEEE in 1982. For 1987 and 1988, he was elected Director of IEEE Division IV, Electromagnetics and Radiation, and thereby served on the IEEE Board of Directors. From 1989 to 1993 he held an appointment on the Army Science Board, Wash. D.C. In 1999 he co-received the Outstanding Paper of the Year Award from the Applied Computational Society (ACES). Currently, Dr. Thiele has a consulting practice with various organizations in the Dayton, OH area.

**Michael "Larkin" Hastriter** received a B.S.E.E. degree in 1993 from Brigham Young University (BYU), an M.S.E.E. degree from the Air Force Institute of Technology (AFIT) in 1997, and a Ph.D. in Electrical Engineering from the University of Illinois, Urbana-Champaign in 2003. After graduating from BYU, he was commissioned in the U.S. Air Force and is now serving on active duty as a major. After completing his doctoral studies, he was appointed as an assistant professor at AFIT teaching in the area of electromagnetics. His research interests include radar cross section prediction, measurement, analysis, and validation as well as scattering centers, bistatic scattering, periodic corrugated waveguides, and stealth technology. He was an aerospace signatures analyst for the National Air Intelligence Center from 1993 to 1996 and served as the chief of the advanced signatures section at the Air Force Information Warfare Center (AFIWC) from 1998 to 1999. He then led the modelling and simulation section and advanced into the position of chief of the signatures branch where he led a team of officers, enlisted, and civil servants as well as directing the efforts of three contractor teams prior to selection for the AFIT faculty pipeline program in 2000. He currently serves as the chief of the electrical engineering division at AFIT. He was awarded the Meritorious Service Medal, Air Force Commendation Medal, Air Force Achievement Medal, and the Military Outstanding Volunteer Service Medal for his military service. He was a distinguished graduate (top 10%) of the Air Force Institute of Technology and at Squadron Officer School and has completed in-residence Air Command and Staff College. He has also been named company grade officer of the quarter (AFIWC) and field grade officer of the quarter (AFIT). He is a member of Tau Beta Pi, Eta Kappa Nu, and a senior member of IEEE. He was a National Collegiate Engineering Awards winner in 2001. He is an Eagle scout and has served as a troop committee chairman, varsity coach, assistant scoutmaster, and a webelos leader. He is projected to become the Deputy Chief for the Air Force Materiel Command CAG (commander's action group) in 2005.

**Michael J. Havrilla** received B.S. degrees in Physics and Mathematics in 1987, the M.S.E.E degree in 1989 and the Ph.D. degree in electrical engineering in 2001 from Michigan State University, East Lansing, MI. From 1990-1995, he was with General Electric Aircraft Engines, Cincinnati, OH and Lockheed Skunk Works, Palmdale, CA, where he worked as an electrical engineer. He joined the Electrical and Computer Engineering Department at the Air Force Institute of Technology as an Assistant Professor in 2002. His current research interests include guided-wave theory, electromagnetic materials characterization, microwave engineering and electromagnetic radiation and scattering.

**Andrew J. Terzuoli** received his Ph.D. from The Ohio State University (OSU) in 1982, his MS from Massachusetts Institute of Technology in 1970, and his BS from Polytechnic Institute of Brooklyn in 1969, all in electrical engineering. He has been on the civilian faculty of the Air Force Institute of Technology since late 1982. Prior to this he was a research associate at the ElectroScience Laboratory at OSU, and a member of the technical staff at the Bell Telephone Laboratories. His research areas include Computer Model Based Studies; Application of Parallel Computation, VLSI Technology, and RISC Architecture to Numerical and Transform Methods in electromagnetics; Remote Sensing and Communication; Passive Radar; Antennas, Electromagnetics, Wave Scattering, Radar Cross Section; Machine Vision and Image Processing; Automated Object Recognition. He has published numerous reports and articles in journals and conference proceedings in these and related areas. His research has been funded by various agencies of the US Government and private industry and research institutes.